

## TETRATAENITE PHASE IN ANTARCTIC METEORITES

Takesi NAGATA and Minoru FUNAKI

National Institute of Polar Research, 9–10, Kaga 1-chome, Itabashi-ku, Tokyo 173

**Abstract:** Four Ni-rich iron meteorites containing tetrataenite ( $\gamma'$ -phase of Fe-Ni metal) and 2 LL chondrites containing the  $\gamma'$ -phase are provisionally selected as the standard  $\gamma'$ -rich meteorites. They are Santa Catharina and Twin City Ni-rich ataxites, taenite lamellae from Toluca and Itutinga octahedrites and St. Séverin and Appley Bridge LL chondrites. The contents of  $\gamma'$ -phase in these standard  $\gamma'$ -rich meteorites were determined by the Mössbauer spectral analysis and their magnetic hysteresis and thermomagnetic characteristics were examined.

The magnetic criteria for  $\gamma'$ -rich meteorites derived from the present study are summarized as follows:

- (1) Remanence coercive force ( $H_{RC}$ ) is anomalously large (*i.e.*  $H_{RC} \geq 500$  Oe).
- (2) The apparent Curie point is 560–580°C.
- (3) The initial heating thermomagnetic (TM) curve of the  $\gamma'$ -phase is flat below about 500°C and then sharply drops down to the apparent Curie point.
- (4) After heating to temperatures above 700°C, the  $\gamma'$ -phase is broken down to the ordinary disordered  $\gamma$ -phase, so that the first-cooling curve and subsequent TM curves have the characteristics of those of  $\gamma$ -phase.
- (5) Because of the break-down of  $\gamma'$ -phase during the heating procedure,  $H_C$  and  $H_{RC}$  are much reduced, by up to one order of magnitude or more from their pre-heating initial values.

In the present experimental study, 5 Antarctic L chondrites and 4 Antarctic LL chondrites are magnetically examined. The Antarctic chondrites which satisfy the five criteria for  $\gamma'$ -rich meteorites are Yamato-74354 (L6), -74362 (L6), -74442 (L6), ALH-76009 (L6) and Y-790964 (LL).

### 1. Introduction

In a previous paper (NAGATA *et al.*, 1986), basic magnetic properties of tetrataenite-rich meteorites, St. Séverin (LL6) and Appley Bridge (LL6) chondrites, and Santa Catharina Ni-rich ataxite, were described in some detail. In addition to these three tetrataenite-rich meteorites, 3 tetrataenite-rich iron meteorites are magnetically analyzed and their contents of tetrataenite are determined by Mössbauer spectral analyses (NAGATA *et al.*, 1987). The additional iron meteorites are Twin City Ni-rich ataxite and taenite lamellae from Toluca and Itutinga octahedrites.

Among the four iron meteorite samples, the Santa Catharina and taenite lamellae from the Toluca and the Itutinga consist of a tetrataenite phase of around a half of the total metal and the ordinary taenite, while the tetrataenite content in the Twin City is about 10%. The tetrataenite content in the Appley Bridge is about 80% while it is about 10% in the St. Séverin. It may be considered therefore that the six meteorite samples are classified into a tetrataenite-rich ataxite, a tetrataenite-containing ataxite, two tetrataenite-rich lamellae from octahedrite, a chondrite containing tetrataenite-rich

metal and a chondrite including tetrataenite-containing metal. On the other hand, basic crystallographic and magnetic properties of a man-made single crystal of the tetrataenite have been well studied by NÉEL *et al.* (1964). According to their experimental results, the lattice parameters of the tetragonal unit cell of this ordered crystal of AuCu type are given by  $a=2.533 \text{ \AA}$  and  $c=3.582 \text{ \AA}$ , and therefore the magnetic anisotropy of this 50Fe50Ni metal is anomalously large, the magnetic coercive force of an assembly of random-oriented crystals of tetrataenite amounting to about  $4 \times 10^3 \text{ Oe}$ .

The petrographical structures of iron meteorites and metallic grains in stony meteorites are complicated so that interactions and diffusive exchanges between neighboring different phases cannot be ignored. In the previous papers (NAGATA *et al.*, 1986, 1987), therefore, basic magnetic properties of the six meteorites containing a considerable amount of tetrataenite phase in different petrographical boundary conditions have been magnetically analyzed.

The magnetic properties of these tetrataenite-containing meteorites commonly exhibit well-defined magnetic characteristics of tetrataenite phase which are established for the man-made single crystal of tetrataenite — 50Fe50Ni in atomic ratio composition. Namely, (a) an unusually high magnetic coercivity in the original pre-heating stage, (b) a break-down of the high coercivity phase by heating to temperature beyond the transformation temperature ( $320^\circ\text{C}$ ) between tetrataenite phase and the ordinary disordered taenite phase, in practice up to temperatures above  $700^\circ\text{C}$  for the purpose of heat treatment of laboratory experimental time duration, and (c) uniquely characteristic shapes of thermomagnetic curves of the initial heating and cooling processes. Each of these characteristic magnetic properties of tetrataenite-rich meteorites have already been qualitatively pointed out for individual cases by several workers (*e.g.* WASILEWSKI, 1982; NAGATA and FUNAKI, 1982, 1983; NAGATA *et al.*, 1986).

In the present study, the characteristic magnetic properties to represent presence of tetrataenite-phase are experimentally examined, as much as quantitatively, on selected new samples of meteorite, in which the content of tetrataenite is determined by means of the Mössbauer spectral analysis or other techniques, and the results are summarized in terms of the criteria for detecting the presence of tetrataenite. The criteria thus obtained are checked on other meteorites which have been proved to contain a fair amount of tetrataenite for the purpose of establishing a reliable scheme of the criteria for detecting the presence of tetrataenite. Then finally, the criteria are applied on Antarctic meteorites in order to search for the presence of the tetrataenite phase in their metallic components.

It has been confirmed that the natural remanent magnetization of tetrataenite-rich meteorites is extremely stable against AF-demagnetization, because of the unusually high magnetic coercivity of tetrataenite (*e.g.* NAGATA and FUNAKI, 1982; NAGATA *et al.*, 1986). It would mean that the magnetization of tetrataenite-containing meteorites is particularly important in the paleomagnetic research of the primordial solar system by use of a large number of meteorites.

In the present note, the tetrataenite phase will be termed the  $\gamma'$ -phase of Fe-Ni metal, for the sake of simplicity, according to RAUTER *et al.* (1985). In comparison, the ordinary disordered taenite will be termed the  $\gamma$ -phase as usual.

## 2. Characteristic Magnetic Properties of Standard $\gamma'$ -rich Meteorites

The metallic phase compositions of Santa Catharina and Twin City Ni-rich ataxites and those of taenite lamellae from Toluca and Itutinga octahedrites, determined by Mössbauer spectral analyses (NAGATA *et al.*, 1987) are summarized in Table 1. The metallic phase compositions of St. Séverin and Appley Bridge LL-chondrites also are summarized in the same table (NAGATA *et al.*, 1986).

Table 1. Metallic phase composition of standard  $\gamma'$ -containing meteorites.

| Meteorite                  | Composition (wt%)     |                      |                            |
|----------------------------|-----------------------|----------------------|----------------------------|
|                            | Kamacite ( $\alpha$ ) | Taenite ( $\gamma$ ) | Tetrataenite ( $\gamma'$ ) |
| Santa Catharina            | $\sim 0$              | 49                   | 51                         |
| Twin City                  | 62                    | 30                   | 8                          |
| Toluca (taenite lamella)   | $\sim 0$              | 36                   | 64                         |
| Itutinga (taenite lamella) | $\sim 0$              | 60                   | 40                         |
| St. Séverin (metal)        | 39.5                  | 51                   | 9.5                        |
| Appley Bridge (metal)      | $\sim 0$              | 20                   | 80                         |

As given in Table 1, the Santa Catharina, the metallic component of the Appley Bridge, and taenite lamellae from the Toluca and the Itutinga consist mostly of  $\gamma$ - and  $\gamma'$ -phases only and the share rate of  $\gamma'$ -phase is about a half or more, while the Twin City and the metallic component of the St. Séverin are composed of  $\alpha$ -phase in addition to  $\gamma$ - and  $\gamma'$ -phases and the  $\gamma'$ -phase is about 10% or less.

The magnetic hysteresis curves for these six standard  $\gamma'$ -containing meteorite samples have been measured at atmospheric temperature for the original pre-heating condition and after heating twice to temperature of 800°C or above in  $10^{-4}$  or less atmospheric pressure. Continuous thermomagnetic (TM) curves for two heating-cooling cycles between ambient temperature and the elevated temperature are measured in an external magnetic field of 10 kOe. Characteristic magnetic properties of these six standard  $\gamma'$ -containing meteorites can be summarized as follows:

### (i) Magnetic hysteresis characteristics

Saturation magnetization ( $I_s$ ), saturated remanent magnetization ( $I_R$ ), coercive force ( $H_C$ ) and remanence coercive force ( $H_{RC}$ ) of the six standard  $\gamma'$ -containing meteorites before and after the heating procedures are summarized in Table 2. A remarkably characteristic feature of the magnetic hysteresis curves of the  $\gamma'$ -containing meteorites is that both  $H_C$  and  $H_{RC}$  in the original pre-heating stage are unusually large,  $H_C$  and  $H_{RC}$  values exceeding 500 and 1000 Oe respectively except for the Appley Bridge, in which  $H_C=160$  Oe and  $H_{RC}=470$  Oe. Ratios  $I_R/I_s$  of these  $\gamma'$ -including meteorites also are unusually large in comparison with the ratio values of most meteorites.

Another remarkable feature is that the anomalously large values of  $H_C$ ,  $H_{RC}$  and  $I_R/I_s$  are extraordinarily reduced by the heat treatment. The heat treatment effect of an extraordinary reduction of magnetic coercivity indicates the high coercivity com-

Table 2. Magnetic hysteresis parameters in pre-heating and post-heating states at atmospheric temperature (20–25°C) and apparent Curie point of  $\gamma'$ -phase for standard  $\gamma'$ -containing meteorite.

| Meteorite                          | $I_s$<br>(emu/g) | $I_R$ | $H_C$<br>(Oe) | $H_{RC}$ | $\theta_C$<br>(°C) |
|------------------------------------|------------------|-------|---------------|----------|--------------------|
| Santa Catharina (pre-heating)      | 81               | 42.5  | 2800          | 4060     | 565                |
| " (post-heating)                   | 105              | 0.23  | 9.5           | 335      |                    |
| Twin City (pre-heating)            | 85               | 42.5  | 760           | 1030     | 560                |
| " (post-heating)                   | 85               | 0.20  | 1.5           | 30       |                    |
| Toluca lamella (pre-heating)       | 111              | 10.8  | 960           | 1950     | 580                |
| " (post-heating)                   | 103              | 2.7   | 8.5           | 33       |                    |
| Itutinga lamella (pre-heating)     | 74               | 39.5  | 2400          | 3830     | 565                |
| " (post-heating)                   | 99.5             | 1.7   | 5             | 30       |                    |
| St. Séverin (bulk) (pre-heating)   | 2.80             | 0.50  | 520           | 1840     |                    |
| " (post-heating)                   | 3.85             | 0.021 | 9.5           | 110      |                    |
| St. Séverin (metal) (pre-heating)  | 142              | 25    | 860           | 2140     | 565                |
| " (post-heating)                   | 125              | 0.20  | 3.5           | 47       |                    |
| Appley Bridge (bulk) (pre-heating) | 1.73             | 0.121 | 160           | 470      | 565                |
| " (post-heating)                   | 2.42             | 0.031 | 14.5          | 73       |                    |

ponent is broken down by the heat treatment,  $\gamma'$ -phase component being transformed to the ordinary  $\gamma$ -phase.

#### (ii) Thermomagnetic characteristics

The first-run and second-run thermomagnetic (TM) curves measured in an external magnetic field of 10 kOe are shown in Fig. 1a for the two  $\gamma'$ -containing ataxites and lamellae from the two  $\gamma'$ -containing octahedrites, and in Fig. 1b for the two  $\gamma'$ -containing LL chondrites.

A remarkable thermomagnetic characteristic, which is consistent for the standard  $\gamma'$ -containing meteorites, is the irreversibility between the first-run heating TM-curve and the first-run cooling TM-curve, where the general features of the first-run cooling TM-curve are approximately followed by the subsequent second-run heating and cooling TM-curves. The first-run heating TM-curve is flat in the temperature range below about 500°C but it sharply drops down to the apparent Curie point (560–580°C) with increasing temperature above 500°C.

The first-run cooling TM-curve can be characterized, on the contrary, by a definitely larger temperature gradient ( $\partial I_s / \partial T$ ) in comparison with that of the first-run heating TM-curve in a temperature range below about 500°C. The TM-curves of the Toluca lamella and the St. Séverin metal are accompanied by a kamacite phase ( $\alpha$ -phase) which is characterized by the  $\alpha \rightarrow \gamma$  transformation in the heating process at 740°C and the  $\gamma \rightarrow \alpha$  transformation in the cooling process at 620°C in the Toluca lamella, while the  $\alpha \rightarrow \gamma$  transformation at 780°C and the  $\gamma \rightarrow \alpha$  transformation at 665°C in the St. Séverin metal. In the case of a Toluca lamella analyzed by Mössbauer spectral method, no  $\alpha$ -phase is attached as shown in Table 1. In the case of another Toluca lamella analyzed magnetically, however, the  $\alpha$ -phase in the Widmannstätten structure of the octahedrite could not be completely removed (NAGATA *et al.*, 1987).

In the TM-curve of the Twin City, on the other hand, no  $\alpha$ -phase ferromagnetic component can be observed in Fig. 1a. In this case, the  $\alpha$ -phase detected by the

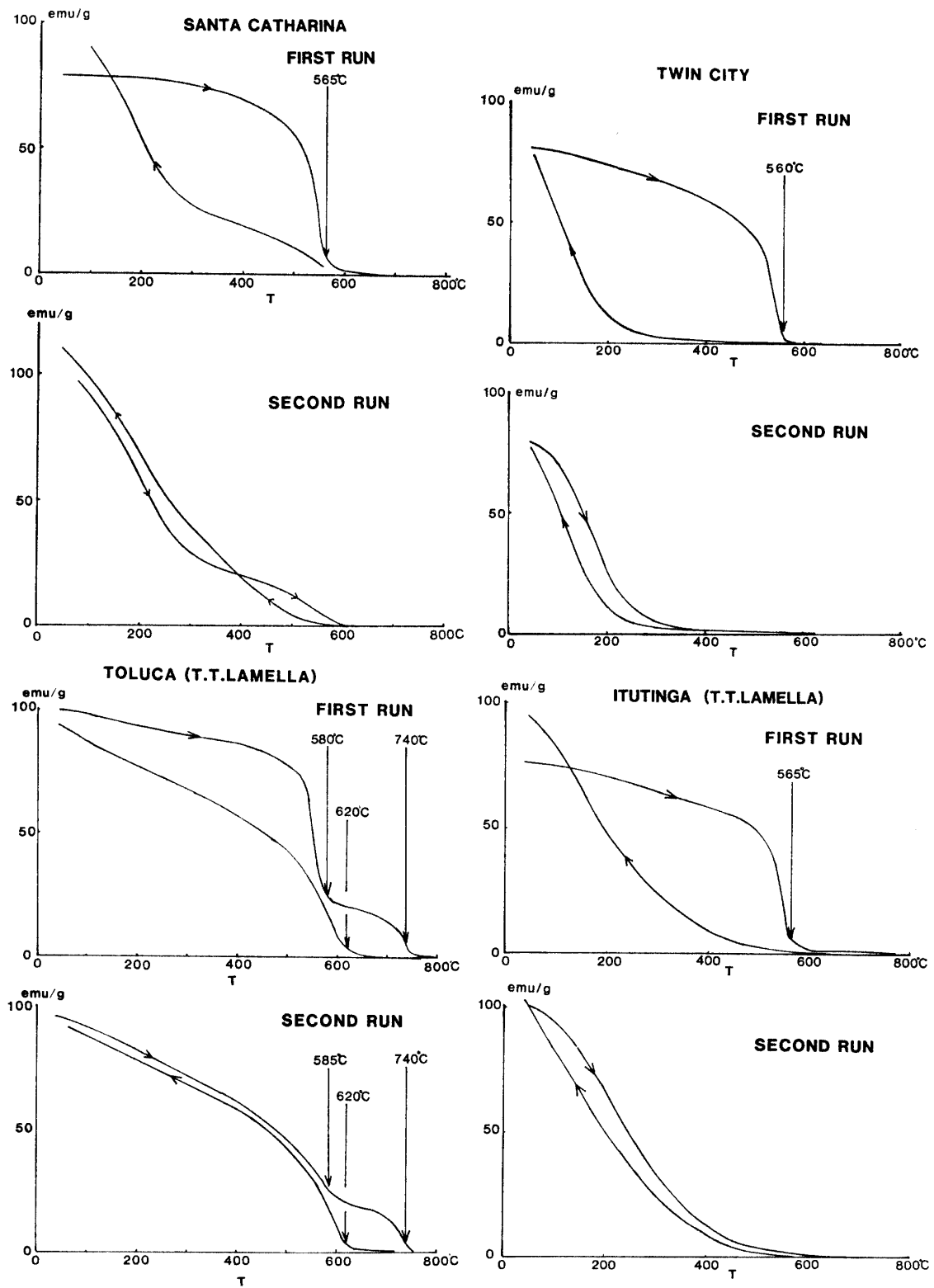


Fig. 1a. The first-run and second-run thermomagnetic curves of 4 standard  $\gamma'$ -rich iron meteorites. Bulk samples of the Santa Catharina and the Twin City, and taenite lamellae of the Toluca and the Itutinga.

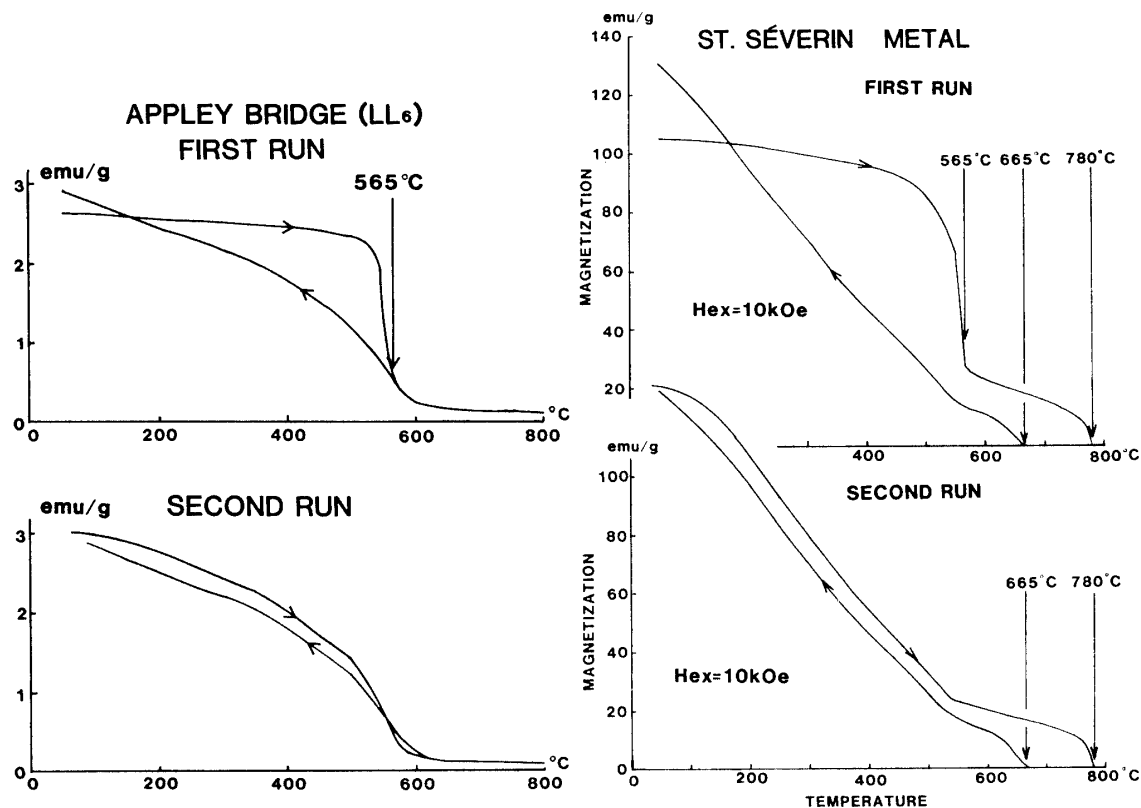


Fig. 1b. The first-run and second-run thermomagnetic curves of 2 standard  $\gamma'$ -rich chondrites. Metal of the St. Séverin and bulk sample of the Appley Bridge.

Mössbauer spectral analysis (Table 1) is identified to a martensitic  $\alpha_2$ -phase of  $M_s = -54^\circ\text{C}$  so that this apparent  $\alpha$ -phase is of a paramagnetic  $\gamma$ -phase in a temperature range above  $20^\circ\text{C}$  (NAGATA *et al.*, 1987).

Apart from the magnetic transition of the associated  $\alpha$ -phase, the observed sharp magnetic transition at  $560\text{--}580^\circ\text{C}$  in all the first-run TM-curves in Fig. 1 may indicate apparent Curie point ( $\theta_c$ ) of  $\gamma'$ -phase or a superimposed component of  $\gamma'$ -phase upon  $\gamma$ -phase. Actually, the TM-curve of the  $\gamma$ -phase 50Fe50Ni (atomic ratio) metal has Curie point at  $560^\circ\text{C}$ , but the TM-curve of  $\gamma'$ -phase of the same composition is nearly flat in a temperature range from 0 K to about 700 K and an extrapolation of the TM-curve looks likely to have Curie Point around 1000 K (NÉEL, private communication). It seems likely therefore that the  $\gamma'$ -phase structure is gradually broken-down to become the  $\gamma$ -phase structure on the heating process beyond  $320^\circ\text{C}$ , and the observed apparent Curie point (about  $560^\circ\text{C}$ ) of the  $\gamma'$ -phase may correspond to Curie point of  $\gamma$ -phase 50Fe50Ni metal.

It may be concluded that the  $\gamma'$ -phase component is broken-down by the heating procedures for TM-curve measurements, being transformed to  $\gamma$ -phase. This conclusion is in agreement with the conclusion obtained by a comparison of the magnetic coercivity of the standard  $\gamma'$ -containing meteorite in the original pre-heating state with that in the post-heating state, summarized in Table 2.

(iii) *Magnetic criteria for identifying  $\gamma'$ -phase*

A summary of characteristic magnetic properties of the standard  $\gamma'$ -containing

meteorites can be itemized as follows:-

(1) Coercive force ( $H_C$ ) and remanence coercive force ( $H_{RC}$ ) are anomalously large ( $H_C \geq 150$  Oe,  $H_{RC} \geq 500$  Oe). As discussed later, the  $H_C$ -value of a binary system consisting of a high coercivity component and a low coercivity component is dominantly controlled to approach the coercive force of the low coercivity component, provided that there is no magnetic interaction among the individual magnetic particles. Therefore, the criterion,  $H_C \geq 150$  Oe, should be considered as a preferable reference condition.

(2) The apparent Curie point of  $\gamma'$ -phase is  $\theta_C = 560$ – $565^\circ\text{C}$ . ( $\theta_C$  could be extended to  $580^\circ\text{C}$ . See Table 2.)

(3) The initial heating TM-curve of  $\gamma'$ -phase is nearly flat in a temperature range below about  $500^\circ\text{C}$  and then sharply decreases to apparent Curie point with increasing temperature.

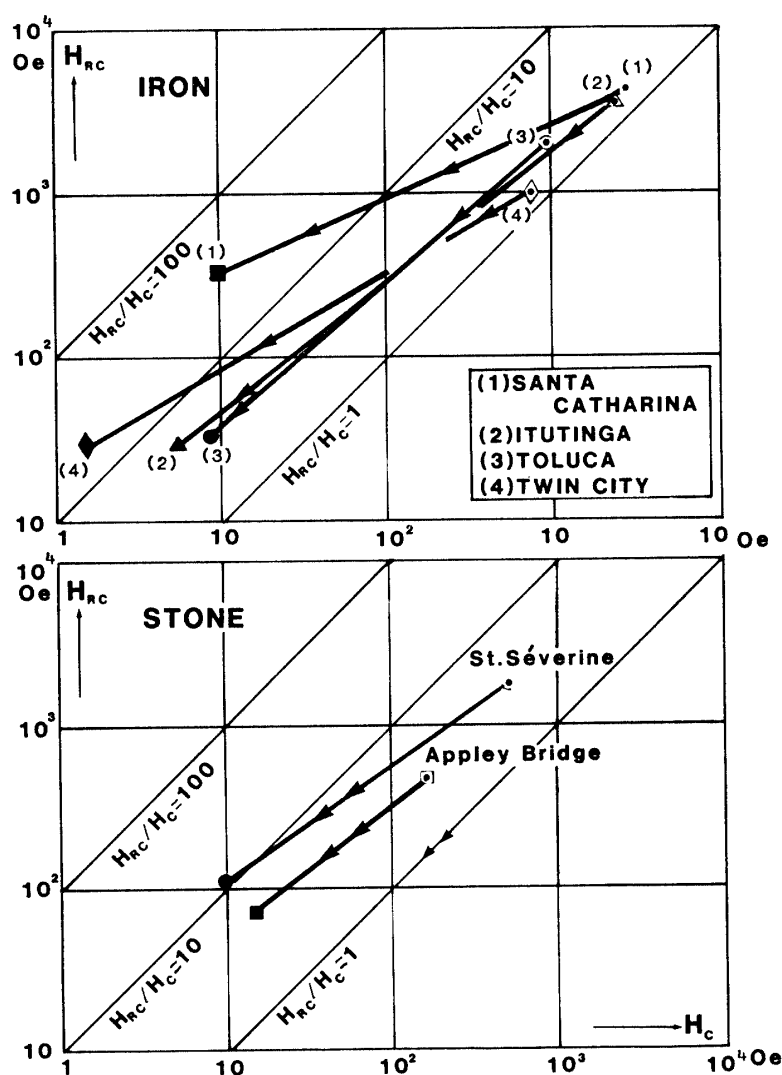


Fig. 2.  $H_{RC}$  vs.  $H_C$  diagrams for expressing a break-down of  $\gamma'$ -phase by heat treatment for standard  $\gamma'$ -rich meteorites.

Top:  $\gamma'$ -rich iron meteorites. Bottom:  $\gamma'$ -rich chondrites.

(4) After heating to temperatures above 700°C,  $\gamma'$ -phase is almost broken down to the ordinary disordered  $\gamma$ -phase. Hence, the first-run cooling and subsequent TM-curves have the characteristics nearly the same as those of  $\gamma$ -phase.

(5) Because of the break down of the  $\gamma'$ -phase by the heating procedure,  $H_C$  and  $H_{RC}$  are much reduced (at least by one order of magnitude) from their respective pre-heating values.

Criteria (1) and (5) in the above can be illustratively combined in a  $H_{RC}$  vs.  $H_C$  diagram, as shown in Fig. 2, where a point ( $H_{RC}$ ,  $H_C$ ) of  $H_{RC}$  in the ordinate and  $H_C$  in the abscissa, both in logarithmic scale, before the heating procedure is connected by an arrow to the post-heating ( $H_{RC}$ ,  $H_C$ ) point for individual samples. In the  $H_{RC}$  vs.  $H_C$  diagrams for the standard  $\gamma'$ -containing meteorites, it is clearly demonstrated that both  $H_{RC}$  and  $H_C$  are reduced at least by one order of magnitude by the heat treatment.

(iv) *Test of the magnetic criteria for identifying  $\gamma'$ -phase*

Two Ni-rich ataxites, the San Cristobal and the Lime Creek, are magnetically analyzed for testing the magnetic criteria for identifying  $\gamma'$ -phase. Since the bulk Ni-contents of the San Cristobal and the Lime Creek are 25.6 and 29.5 wt% respectively, both Ni-rich ataxites appear to have approximately equal possibility of containing  $\gamma'$ -phase.

As for the criteria (1) and (5),  $H_C$ ,  $H_{RC}$  and  $I_R/I_S$  values before and after heating twice to 800°C of these two ataxites are expressed in form of (pre-heating value)→(post-heating value) as

(San Cristobal):  $H_C=185\rightarrow 23$  Oe,  $H_{RC}=3100\rightarrow 160$  Oe,

$I_R/I_S=0.058\rightarrow 0.013$ ,

(Lime Creek):  $H_C=20\rightarrow 12$  Oe,  $H_{RC}=120\rightarrow 150$  Oe,

$I_R/I_S=0.021\rightarrow 0.010$ .

Therefore, the San Cristobal satisfies both criteria (1) and (5), while the Lime Creek neither of them.

As for criterion item (2),  $\theta_C=560\text{--}565^\circ\text{C}$  for the San Cristobal and  $\theta_C=400\text{--}600^\circ\text{C}$  for the Lime Creek. Further the TM-curves of the San Cristobal satisfy both criteria (3) and (4), while all the first-run heating and subsequent TM-curves of the Lime Creek exhibit approximately reversible TM-curves of  $\gamma$ -phase having a wide dispersion of Curie point in a range of 400–600°C, whence criterion (3) is not satisfied.

In concluding, the San Cristobal satisfies all the magnetic criteria for containing  $\gamma'$ -phase while the Lime Creek does not satisfy any one of the five criteria. Results of Mössbauer spectral analyses of these two ataxites indicate that the San Cristobal contains  $\gamma'$ -phase of 8 wt%, while the Lime Creek consists of dominant  $\gamma$ -phase and a small amount of  $\alpha$ -phase, containing practically no  $\gamma'$ -phase (NAGATA *et al.*, 1987).

### 3. $\gamma'$ -rich Antarctic Chondrite

Since the chemical composition of the stoichiometric tetrataenite is 50Fe50Ni in atomic ratio (*i.e.* 48.8Fe51.2Ni in weight), the bulk Ni-content in metallic components of  $\gamma'$ -containing meteorites will be larger than 8 wt% so that the metallic components



have the octahedrite structure consisting of both b.c.c. and f.c.c. phases or the Ni-rich ataxite structure of f.c.c. phase alone.

As the chemical analysis data of Yamato meteorites (HARAMURA *et al.*, 1983) show that the Ni-content in metal is larger than 13.0 wt% in 24 analyzed Yamato L chondrites and larger than 21.0 wt% in 16 analyzed Yamato LL chondrites, Antarctic L and LL chondrites are selected in the present study as possible candidates for the  $\gamma'$ -rich chondrite. Among 5 Antarctic L chondrites and 4 Antarctic LL chondrites which are magnetically analyzed in the present first-stage study, 3 L chondrites and 2 LL chondrites look likely to satisfy the required magnetic criteria (1)–(5) for  $\gamma'$ -rich meteorite; they are Yamato-74354 (L6) and -74362 (L6), ALH-76009 (L6), Y-74442 (LL4) and -790964

Table 3. Content and chemical composition of metallic component of  $\gamma'$ -rich Yamato chondrites.

| Meteorite     | Total metal (wt%) | Fe <sup>o</sup> | Ni <sup>o</sup> (wt%) | Co <sup>o</sup> |
|---------------|-------------------|-----------------|-----------------------|-----------------|
| Y-74354 (L6)  | 7.24              | 6.04            | 1.16                  | 0.040           |
| Y-74362 (L6)  | 7.77              | 6.65            | 1.08                  | 0.040           |
| Y-74442 (LL4) | 3.49              | 2.48            | 0.99                  | 0.015           |
| Y-790964 (LL) | 1.10              | 0.37            | 0.71                  | 0.024           |

Table 4. Magnetic hysteresis parameters at 20–25°C.

| (a) Y-74354 (L6)              |                  |       |               |          |
|-------------------------------|------------------|-------|---------------|----------|
|                               | $I_s$<br>(emu/g) | $I_R$ | $H_C$<br>(Oe) | $H_{RC}$ |
| Original (pre-heating)        | 21.8             | 0.71  | 66            | 2620     |
| After 2nd heating to 890°C    | 19.8             | 0.085 | 11            | 165      |
| After 3rd heating to 890°C    | 19.6             | 0.040 | 5             | 50       |
| (b) Y-74362 (L6)              |                  |       |               |          |
| Original (pre-heating)        | 9.5              | 0.36  | 84            | 2000     |
| After 2nd heating to 820°C    | 11.4             | 0.03  | 6             | 245      |
| After 3rd heating to 820°C    | 11.4             | 0.025 | 6             | 255      |
| (c) Y-790964 (LL shocked)     |                  |       |               |          |
| Original (pre-heating)        | 1.80             | 0.113 | 143           | 550      |
| After 1st heating to 950°C    | 2.69             | 0.014 | 24            | 140      |
| After 2nd heating to 910°C    | 2.60             | 0.015 | 14            | 90       |
| (d) Y-74442 (LL4)             |                  |       |               |          |
| Original (pre-heating)        | 6.3              | 0.23  | 85            | 460      |
| After 1st heating to 850°C    | 6.5              | 0.040 | 10            | 185      |
| After 2nd heating to 840°C    | 6.5              | 0.040 | 10.5          | 230      |
| (e) ALH-76009 (L6) Specimen A |                  |       |               |          |
| Original (pre-heating)        | 18.1             | 0.31  | 35            | 1880     |
| After 2nd heating to 880°C    | 17.3             | 0.075 | 7             | 110      |
| Specimen B                    |                  |       |               |          |
| Original (pre-heating)        | 9.8              | 0.37  | 110           | 2470     |
| After 2nd heating to 900°C    | 9.35             | 0.043 | 10            | 130      |

(LL). The contents of metallic elements in the 4 Yamato meteorites are summarized in Table 3 (HARAMURA *et al.*, 1983). Characteristics of the magnetic hysteresis curves before and after the heating and the TM-curves of the five Antarctic chondrites are summarized in the followings for comparison with those of the present standard  $\gamma'$ -rich meteorites.

### 3.1. Yamato-74354 (L6)

The magnetic hysteresis parameters,  $I_s$ ,  $I_R$ ,  $H_C$  and  $H_{RC}$ , in the original state before heating, after heating twice to 890°C and after the third heating to 890°C are summarized in Table 4a, and TM-curves of the first and second-runs are shown in Fig. 3a.

In these results, the criteria for  $\gamma'$ -containing meteorites (3), (4) and (5) are fully satisfied. Although  $H_{RC}$  value (2620 Oe) in the original state is sufficiently large enough to represent  $\gamma'$ -phase,  $H_C$  value (66 Oe) in the original state is considerably smaller than the preferable  $H_C$  value for a  $\gamma'$ -rich meteorite. As shown by the first-run heating TM-curve in Fig. 3a, a possible content of  $\gamma'$ -phase (represented by  $\theta_c = 543^\circ\text{C}$ ) is much smaller than the other ferromagnetic component which is  $\alpha$ -phase of 6.1 wt% Ni represented by the  $\alpha \rightarrow \gamma$  transition temperature ( $\theta_{\alpha \rightarrow \gamma}^* = 750^\circ\text{C}$ ) and the  $\gamma \rightarrow \alpha$  transition temperature ( $\theta_{\alpha \rightarrow \gamma}^* = 625^\circ\text{C}$ ). In such a case that an extremely high-coercivity component is mixed with a low-coercivity component, the bulk  $H_C$  value

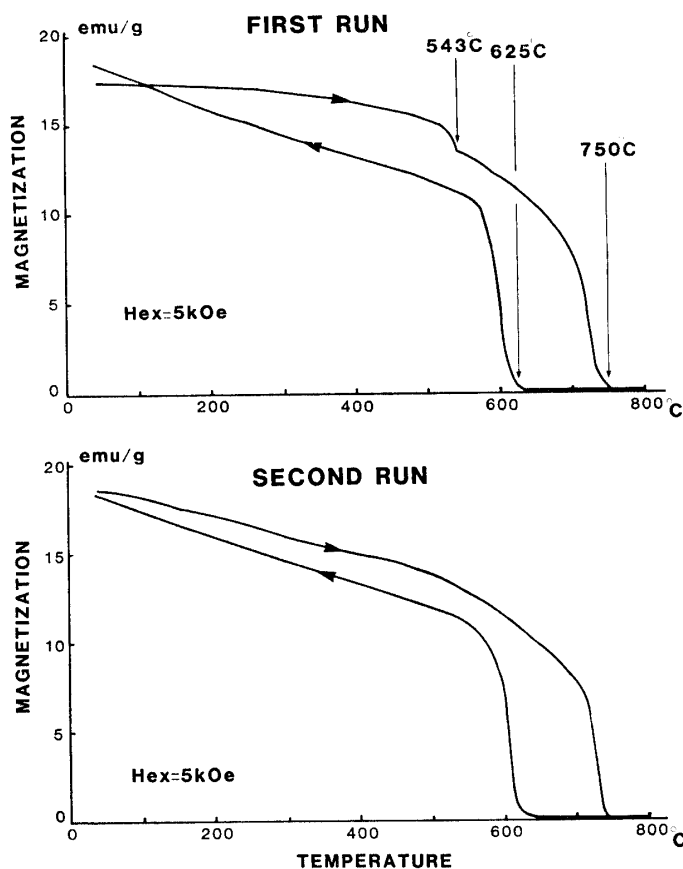


Fig. 3a. The first-run and second-run thermomagnetic curves of Y-74354 L6 chondrite.

of the mixed binary system is strongly controlled by the low-coercivity component to be drawn down to the low-coercive value, while the bulk  $H_{RC}$  value is drawn closer to the high-coercive value provided that there is no magnetic interaction among individual magnetic constituent particles (NAGATA and CARLETON, 1987). According to a theoretical model of the binary system with no magnetic interaction among individual magnetic particles (NAGATA and CARLETON, 1987), remanence coercive force ( $H_{RC}^{(h)}$ ) and coercive force ( $H_C^{(h)}$ ) of the high coercivity component and remanence coercive force ( $H_{RC}^{(l)}$ ) and coercive force ( $H_C^{(l)}$ ) of the low coercivity component for Yamato-74354 are derived from its observed values of  $I_S$ ,  $I_R$ ,  $H_C$  and  $H_{RC}$  as

$$H_{RC}^{(h)} = 2790 \text{ Oe}, \quad H_C^{(h)} = 1860 \text{ Oe},$$

$$H_{RC}^{(l)} = 49 \text{ Oe}, \quad H_C^{(l)} = 12 \text{ Oe},$$

and the content ( $m$ ) of the high coercivity component in the total metal in this chondrite is estimated as  $m=6.2\%$ . The observed large reduction of  $I_R$ ,  $H_C$  and  $H_{RC}$  by the heating procedures would be strong evidence for breaking down of  $\gamma'$ -phase existing in the original pre-heating stage. The proposed expression of break-down phenomena of  $\gamma'$ -phase on a  $H_{RC}$  vs.  $H_C$  diagram for Y-74354 (Fig. 4) may well present the observed changes of  $H_C$  and  $H_{RC}$  by the heating procedure.

Another problem would be concerned with the observed value of apparent Curie point ( $\theta_C=543^\circ\text{C}$ ). As Curie point of  $\gamma$ -phase of 51%Ni is  $505^\circ\text{C}$ , an observed deviation of the  $\theta_C$  value from  $\theta_C=560\text{--}565^\circ\text{C}$  as the standard value may still be allowable

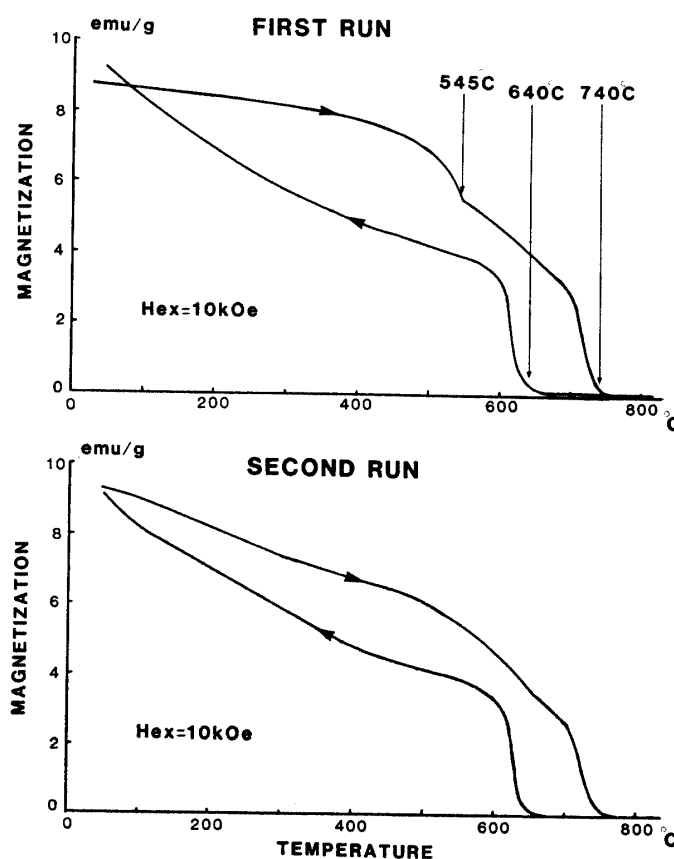


Fig. 3b. The first-run and second-run thermomagnetic curves of Y-74362 L6 chondrite.

for  $\gamma'$ -phase. It seems very likely for a conclusion that Y-74354 metallic component consists of 6 wt% Ni  $\alpha$ -phase of 94% and  $\gamma'$ -phase of 6%.

### 3.2. Yamato-74362 (L6)

Table 4b and Fig. 3b give respectively the magnetic hysteresis characteristics before and after the heating procedures and the first-run and second-run TM-curves of Y-74362.  $I_R/I_S$ ,  $H_C$  and  $H_{RC}$  of Y-74362 before and after the heating procedures are similar to those of Y-74354, though the Fe-Ni metal content, represented by  $I_S$  value, of the former is about a half of that of the latter.

As shown in the  $H_{RC}$  vs.  $H_C$  diagram (Fig. 4),  $H_C$  and  $H_{RC}$  of Y-74362 also markedly decrease after the heating procedures. It seems likely in the case of this chondrite that the break-down of  $\gamma'$ -phase by heating is almost completed by the second heating procedure.

General features of TM-curve characteristics shown in Fig. 3b also are similar to those of Y-74354 (Fig. 3a), consisting of  $\gamma'$ -phase with  $\theta_C=545^\circ\text{C}$  and  $\alpha$ -phase with  $\theta_{\alpha \rightarrow \gamma}^*=740^\circ\text{C}$  and  $\theta_{\gamma \rightarrow \alpha}^*=640^\circ\text{C}$  (corresponding to 5.9 wt% Ni  $\alpha$ -phase).

It may thus be concluded that Y-74362 fully satisfy criteria (3), (4) and (5) and reasonably satisfy criteria (1) and (2), as in the case of Y-74354. The analysis of Y-74362 with the same Nagata-Carleton method as applied on Y-74354 have led to results that  $H_{RC}^{(h)}=1380$  Oe,  $H_C^{(h)}=920$  Oe,  $H_{RC}^{(1)}=30$  Oe,  $H_C^{(1)}=7$  Oe and  $m=6.3\%$ . The

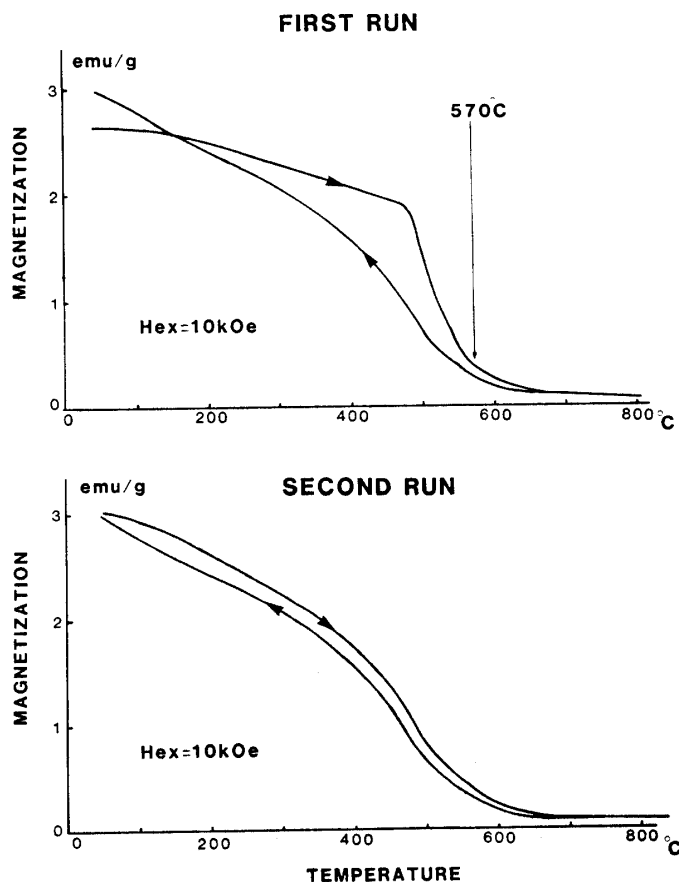


Fig. 3c. The first-run and second-run thermomagnetic curves of Y-790964 LL chondrite.

magnetic composition of Y-74362 is very similar to that of Yamato-74354, suggesting that these two L6 chondrites might be fragments of a single meteorite body.

### 3.3. Yamato-790964 (LL shocked)

The magnetic hysteresis characteristics and TM-curves of Y-790964 are given in Table 4c and Fig. 3c respectively, and its  $H_{RC}$  vs.  $H_C$  diagram is shown in Fig. 4. The observed magnetic properties of this LL chondrite sufficiently satisfy criteria (2), (3), (4) and (5), and satisfy the lower limit of criterion item (1) for a  $\gamma'$ -containing meteorite.

As given in Table 3, the metallic component of Y-790964 is extremely Ni rich, suggesting that the metallic component is mostly taenite, *i.e.*  $\gamma'$ -phase and  $\gamma$ -phase. The observed relatively small values of  $H_C$  and  $H_{RC}$  in comparison with these parameters of  $\gamma'$ -rich iron meteorites suggest that the original taenite in metal comprises minor  $\gamma'$ -phase and abundant  $\gamma$ -phase.

The observed values of  $I_S$ ,  $I_R$ ,  $H_C$  and  $H_{RC}$  before and after the heating procedures of Y-790964 are closely similar to those of Appley Bridge LL chondrite.

### 3.4. Yamato-74442 (LL4)

The magnetic hysteresis characteristics and TM-curves of Y-74442 are shown in Table 4d and Fig. 3d respectively, and the  $H_{RC}$  vs.  $H_C$  diagram in Fig. 4 illustrates the breaking-down change of its magnetic coercivity by the heating procedure.

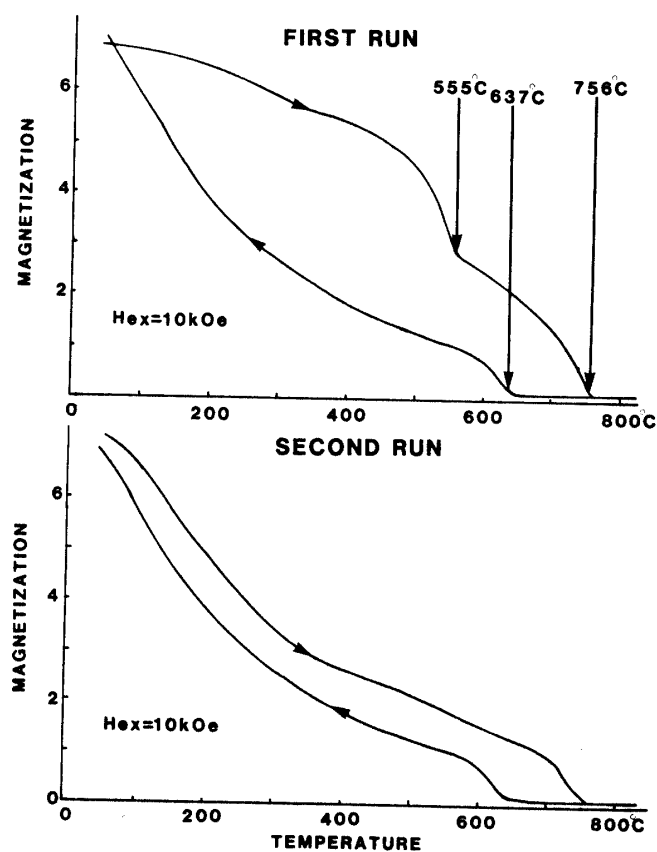


Fig. 3d. The first-run and second-run thermomagnetic curves of Y-74442 LL4 chondrite.

The observed magnetic properties of this chondrite before and after the heating procedures well satisfy criteria (2), (3), (4) and (5) for  $\gamma'$ -containing meteorite.  $H_{RC}$  in the original pre-heating stage is a little smaller than its standard value, but the  $H_{RC}$ -value is nearly the same as that of the Appley Bridge. Both Y-790964 and -74442 chondrites are picked up in the present study as possible examples of the  $\gamma'$ -containing Antarctic chondrites, mostly because their magnetic characteristics are closely similar to those of the Appley Bridge chondrite. However, the physical mechanism for causing the observed small value of  $H_{RC}$  ( $H_{RC}=490$  Oe) of the Appley Bridge has not yet been satisfactorily clarified. If the magnetic interaction among individual magnetic constituents is negligibly small, as assumed in the Nagata-Carleton binary system model, the  $H_{RC}^{(h)}$  value of the high coercivity component is estimated to be about 500 Oe in the case of the Appley Bridge. If, on the other hand, small grains of  $\gamma'$ -phase are closely surrounded by the low coercivity metals, it is possible that the effective magnetic field for the  $\gamma'$ -phase grains is intensified by the magnetic interaction effect. This possible effect may result in a considerable decrease in the observed values of both  $H_{RC}^{(h)}$  and  $H_C^{(h)}$ . The problem of possible magnetic interaction effect among ferromagnetic metallic phases has not yet been quantitatively solved for stony meteorites.

An analysis of the TM-curves having the  $\theta_{\alpha \rightarrow \gamma}^*=756^\circ\text{C}$ ,  $\theta_{\gamma \rightarrow \alpha}^*=637^\circ\text{C}$  and  $\theta_C=555^\circ\text{C}$  suggests that the Ni-content of  $\alpha$ -phase is 5.9 wt% and the weight contents of both  $\alpha$ -phase and  $(\gamma'+\gamma)$ -phase are about 50%.

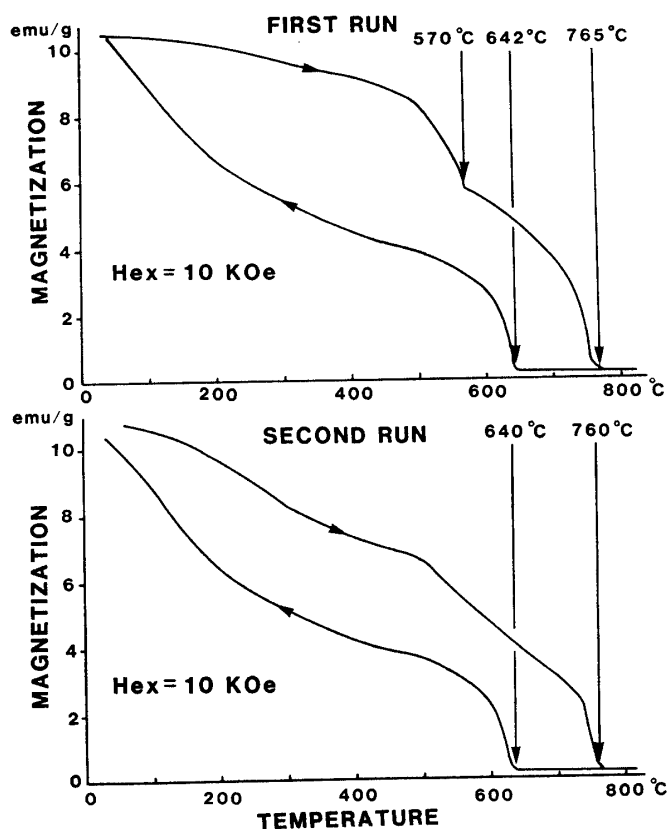


Fig. 3e. The first-run and second-run thermomagnetic curves of ALH-76009 L6 chondrite.

### 3.5. ALH-76009 (L6)

As shown by TM-curves in Fig. 3e, the metallic component of ALH-76009 L6 chondrite consists of  $\alpha$ -phase and  $\gamma'$ -phase (and  $\gamma$ -phase). The magnetic hysteresis characteristics before and after the heating are summarized in Table 4e for two test specimens, A and B.

Although  $I_s$  values of A and B specimens are considerably different from each other, the magnetic properties of both specimens satisfactorily satisfy criteria (2), (3), (4) and (5) and also the pre-heating  $H_{RC}$  value for criterion (1) for the  $\gamma'$ -containing meteorite. The observed reduced value of  $H_C$  (in particular for Specimen A) in the original pre-heating stage is attributable to the co-existence of multidomain  $\alpha$ -phase and  $\gamma$ -phase.

An analysis of TM-curves of ALH-76009 of  $\theta_{\alpha \rightarrow \gamma}^* = 765^\circ\text{C}$ ,  $\theta_{\gamma \rightarrow \alpha}^* = 642^\circ\text{C}$  and  $\theta_C = 570^\circ\text{C}$  leads to conclusions that the Ni-content of  $\alpha$ -phase is 5.9 wt% and that the weight contents of  $\alpha$ -phase and ( $\gamma' + \gamma$ )-phase are about 56 and 44% respectively. It may thus be concluded that the metallic component of ALH-76009 consists of  $\alpha$ -,  $\gamma'$ - and  $\gamma$ -phases, where the content of  $\gamma'$ -phase is considerably smaller than 44 wt%. If the Nagata-Carleton model of the binary system is applied on ALH-76009 Specimen B by assuming that the sum of the  $\alpha$ - and the  $\gamma$ -phases can be considered as a single low coercivity component, we can get  $H_{RC}^{(h)} = 2530$  Oe,  $H_C^{(h)} = 1680$  Oe,  $H_{RC}^{(1)} = 76$  Oe,  $H_C^{(1)} = 19$  Oe and  $m = 7.2\%$ .

Table 5. Magnetic hysteresis characteristic parameters of bulk, chondrules, matrices and metallic grains of ALH-76009 chondrite.

| Component | Number of sample | $I_s$<br>(emu/g) | $I_R$       | $H_C$<br>(Oe) | $H_{RC}$  |
|-----------|------------------|------------------|-------------|---------------|-----------|
| Bulk      | 4                | 8.4–18.1         | 0.31–0.52   | 35–160        | 1880–2700 |
| Chondrule | 6                | 0.99–3.67        | 0.012–0.091 | 45–176        | 940–2650  |
| Matrix    | 3                | 5.7–12.8         | 0.27–0.80   | 45–132        | 1140–2610 |
| Metal     | 5                | 81–171           | 0.18–0.53   | 1.0–13.5      | 60–150    |

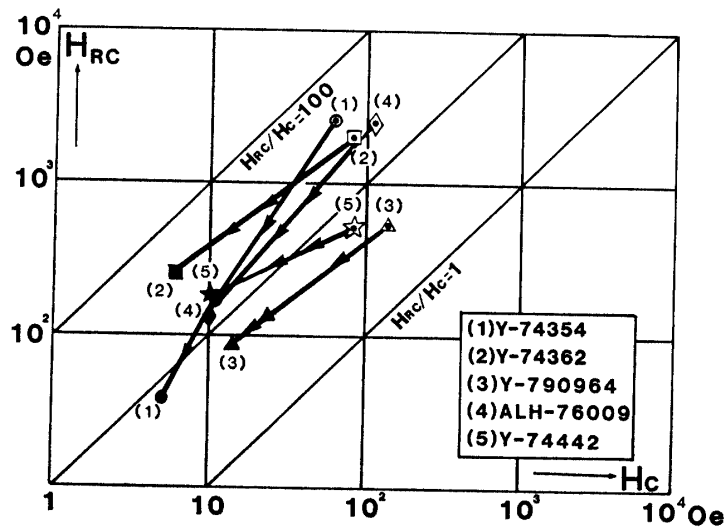


Fig. 4.  $H_{RC}$  vs.  $H_C$  diagram of 5 Antarctic  $\gamma'$ -containing chondrites.

As suggested by a considerable difference of  $I_s$  values between A and B specimens, the distribution of metallic grains in this chondrite is not uniform. The original pre-heating values of  $I_s$ ,  $I_R$ ,  $H_C$  and  $H_{RC}$  of bulk specimens, chondrules, matrix and metallic grains of ALH-76009 chondrite are separately measured, the results being summarized in Table 5 (NAGATA and FUNAKI, 1981). In comparison of Table 4e with Table 5, it will be obvious that the high magnetic coercivity represented by a large value of  $H_{RC}$  of the bulk specimen is mostly due to matrix and chondrules which contain fine particles of  $\gamma'$ -rich metal, while the bulk  $I_s$  value is largely due to the content of larger metallic grains of low coercivity.

### 3.6. Examples of other chondrites having no magnetic evidence for the $\gamma'$ -containing meteorites

Magnetic properties of some other L chondrites do not satisfy the present criteria for  $\gamma'$ -containing meteorite. For example, Y-74190 (L5-6) chondrite has the magnetic hysteresis characteristics such as  $I_R/I_s=0.0022$ ,  $H_C=6$  Oe and  $H_{RC}=91$  Oe, and its TM-curves have no definite indication of a magnetic transition at 560–570°C, though its contents of metallic elements are 6.55% Fe°, 1.11% Ni° and 0.04% Co° in weight, (i.e. 14.4 wt% Ni in metal) (HARAMURA *et al.*, 1983). Y-75110 (L4) chondrite also has similar magnetic properties such as  $I_R/I_s=0.0064$ ,  $H_C=9$  Oe and  $H_{RC}=93$  Oe, though its contents of metallic elements are 7.09% Fe°, 1.05% Ni° and 0.04% Co° in weight (i.e. 12.8 wt% Ni in metal) (HARAMURA *et al.*, 1983). Neither Y-74190 nor -75110 satisfies the criteria (1), (2) and (3).

An example of another group of chondrites which do not fulfil the proposed criteria for the  $\gamma'$ -containing meteorite is Y-790250 (LL4) chondrite. Magnetic properties of this LL chondrite in the original pre-heating stage are given by  $I_R/I_s=0.026$ ,  $H_C=78$  Oe, and  $H_{RC}=620$  Oe, and in its first-run TM-curve,  $\theta_C=570^\circ\text{C}$  and there is no magnetic transition of  $\alpha$ -phase. It appears therefore that the criterion (1) is nearly satisfied and criterion (2) is sufficiently satisfied. However, the hysteresis parameters after heating twice to 850°C become  $I_R/I_s=0.15$ ,  $H_C=154$  Oe and  $H_{RC}=355$  Oe. Namely, magnetic characteristics regarding to criteria (3), (4) and (5) in this chondrite are not satisfied compared with other  $\gamma'$ -containing meteorites. In particular, large increases of  $H_C$  and  $I_R/I_s$  values caused by the heating procedures in this chondrite are opposite in the sense of change to those in  $\gamma'$ -rich meteorites.

A similar example is Y-790448 (LL3) chondrite. In this case,  $I_R/I_s=0.023$ ,  $H_C=63$  Oe and  $H_{RC}=680$  Oe in its original pre-heating stage. After heating twice to 830°C, these hysteresis parameters change to  $I_R/I_s=0.10$ ,  $H_C=175$  Oe and  $H_{RC}=450$  Oe, just as in the case of Y-790250. In regard to TM-curve characteristics,  $\theta_{\alpha\rightarrow\gamma}^*=770^\circ\text{C}$  and  $\theta_{\gamma\rightarrow\alpha}^*=720^\circ\text{C}$  for the  $\alpha$ -phase in addition to  $\theta_C=575^\circ\text{C}$  for the  $\gamma$ -phase in the first-run TM-curves, and the second-run TM-curves are roughly similar to the first-run TM-curves, indicating no evidence for a break-down of  $\gamma'$ -phase. The contents of metallic elements in Yamato-790448 are given by 1.33% Fe°, 0.90% Ni° and trace of Co° in weight, (HARAMURA *et al.*, 1983). Since the average Ni-content in the metal is estimated to be 40% and the metallic component consists of  $\alpha$ -phase and  $\gamma$ -phase in this LL chondrite, the Ni-content in the taenite phase is around 50% or more. Nevertheless, no evidence for presence of  $\gamma'$ -phase is detected in this LL chondrite.



#### 4. Concluding Remarks

Although some chondrites containing Ni-rich metallic grains such as Yamato-790250 and -790448 contain no or a very small amount of  $\gamma'$ -phase, some other L and LL chondrites often contain relatively Ni-rich metallic grains including  $\gamma'$ -phase, which can be magnetically identified as in the present study.

It has been reported by DANON *et al.* (1979), on the other hand, that the presence of a fair amount (36.6–50.8%) of  $\gamma'$ -phase in the metallic component of the Lake Labyrinth (LL6), the Parambu (LL5) and the St. Séverin (LL6), and a less but considerable amount (7.8–17.4%) of  $\gamma'$ -phase in metallic component of the L'Aigle (L4), the Björbole (L4), the Peetz (L6) and the Shaw (L6), are identified by Mössbauer spectral analyses.

CLARKE and SCOTT (1980) also reported that they could optically identify the "clear taenite" phase, which is very likely to be identical to  $\gamma'$ -phase, in 15 H chondrites, 8 L chondrites and 9 LL chondrites in addition to a number of iron and stony-iron meteorites.

In the present stage of systematically searching for the  $\gamma'$ -phase in Antarctic stony meteorites on the basis of their magnetic properties, it seems likely that 3 L chondrites and 2 LL chondrites can be identified as  $\gamma'$ -rich (or  $\gamma'$ -containing) chondrites with satisfactory reliability. Further studies on many other Antarctic L and LL chondrites will be needed in order to examine a statistical rate of existence of  $\gamma'$ -phase in chondrites in general.

As discussed in regard to the magnetic coercivity of Antarctic L and LL chondrites, it seems that the proposed criterion (1) for  $H_{RC}$  and  $H_C$  values in the original pre-heating stage as one of evidence for the  $\gamma'$ -containing meteorites may have to be examined in more detail, experimentally and theoretically, by taking into consideration the possible effect of the magnetic interaction among individual magnetic phases. Since a test sample for the present magnetic measurements of the Appley Bridge was not the same sample as the Appley Bridge test sample for the Mössbauer spectral analysis (NAGATA *et al.*, 1986), a possibility that the relative contents of  $\gamma$ - and  $\gamma'$ -phases in metals are different between the two test samples may not be rejected. It is hoped therefore that careful synthetic studies on the micro-structure of  $\gamma'$ -containing metallic grains and their magnetic properties, including those of the Appley Bridge, will be undertaken in the future. It would be emphasized here that all the proposed magnetic criteria, from (1) through (5), must be satisfied for verifying existence or co-existence of the  $\gamma'$ -phase in meteorites. In particular, it seems that criteria (3), (4) and (5) are extremely significant.

The processes of production and growth of  $\gamma'$ -phase in metallic components in meteorites may sensitively depend upon their thermal history as well as the Ni-content in the meteorites. It may be worth noting in this regard that no clear evidence for presence of  $\gamma'$ -phase in metal has been detected in 23 Antarctic achondrites (10 eucrites, 1 howardite, 8 diogenites and 4 ureilites) so far magnetically analyzed by the present authors. It may be presumed that the  $\gamma'$ -phase in metallic components in the original materials, if any, might have been broken down during the course of their brecciation.

This research work is partly aided by the academic research encouragement fund

from the Japan Academy.

### References

- CLARKE, R. S., Jr. and SCOTT, E. R. D. (1980): Tetrataenite—ordered FeNi, a new mineral in meteorites. *Am. Mineral.*, **65**, 624–630.
- DANON, J., SCORZELLI, R. B., SOUZA AZEVEDO, I. and CHRISTOPHE-MICHEL-LÉVEY, M. (1979): Iron-nickel superstructure in metal particles of chondrites. *Nature*, **281**, 469–471.
- HARAMURA, H., KUSHIRO, I. and YANAI, K. (1983): Chemical composition of Antarctic meteorites I. *Mem. Natl Inst. Polar Res., Spec. Issue*, **30**, 109–121.
- NAGATA, T. and FUNAKI, M. (1981): The composition of natural remanent magnetization of an Antarctic chondrite, ALHA76009 (L6). *Proc. Lunar Planet. Sci. Conf.*, **12B**, 1229–1241.
- NAGATA, T. and FUNAKI, M. (1982): Magnetic properties of tetrataenite-rich stoney meteorite. *Mem. Natl Inst. Polar Res., Spec. Issue*, **25**, 222–250.
- NAGATA, T. and FUNAKI, M. (1983): Magnetic analysis of an Antarctic mesosiderite, ALH-77219. *Nankyoku Shiryô (Antarct. Rec.)*, **79**, 1–10.
- NAGATA, T. and CARLETON, B. J. (1987): Magnetic remanence coercivity of rocks. *J. Geomagn. Geoelectr.* (in press.)
- NAGATA, T., FUNAKI, M. and DANON, J. (1986): Magnetic properties of tetrataenite-rich meteorites, II. *Mem. Natl Inst. Polar Res., Spec. Issue*, **41**, 364–381.
- NAGATA, T., DANON, J. and FUNAKI, M. (1987): Magnetic properties of Ni-rich iron meteorites. *Mem. Natl Inst. Polar Res., Spec. Issue*, **46**, 263–282.
- NÉEL, L., PAULEVE, J., PAUTHENET, R., LANGIER, J. and DAUTREPPE, D. (1964): Properties of an iron-nickel single crystal ordered by neutron bombardment. *J. Appl. Phys.*, **35**, 873–876.
- RAUTER, K. B., WILLIAMS, D. B. and GOLDSTEIN, J. I. (1985): A contribution to the low temperature Fe-Ni phase diagram. *Meteoritics*, **20**, 742–743.
- WASILEWSKI, P. J. (1982): Magnetic characterization of tetrataenite and its role in the magnetization of meteorite (abstract). *Lunar and Planetary Science XIII*. Houston, Lunar Planet. Inst., 843–844.

(Received August 14, 1986; Revised manuscript received January 23, 1987)